Published in final edited form as:
J Comp Neurol. 2003 November 10; 466(2): 230–239. doi:10.1002/cne.10872.

Intercellular Interactions in the Mammalian Olfactory Nerve

KAREN J. BLINDER[1,2], **DAVID W. PUMPLIN**[1], **D.L. PAUL**[3], and **ASAF KELLER**[1,*]

[1]Department of Anatomy and Neurobiology, Program in Neuroscience, University of Maryland School of Medicine, Baltimore, Maryland 21201

[2]Department of Anatomy, Howard University College of Medicine, Washington, DC 20059

[3]Department of Neurobiology, Harvard Medical School, Boston, Massachusetts 02115

Abstract

The small, unmyelinated axons of olfactory sensory neurons project to the olfactory bulb in densely packed fascicles, an arrangement conducive to axo-axonal interactions. We recently demonstrated ephaptic interactions between these axons in the olfactory nerve layer, the layer of the olfactory bulb in which the axon fascicles interweave and rearrange extensively. In the present study, we hypothesized that the axons, which express connexins, may have another mode of communication: gap junctions. Previous transmission electron microscopy (TEM) studies have failed to demonstrate such junctions. However, the definitive method for detecting gap junctions, freeze fracture, has not been used to examine the interaxonal connections of the olfactory nerve layer. Here, we apply a combined approach of TEM and freeze fracture to determine if gap junctions are present between the olfactory axons. Gap junctions involving olfactory axons were not found. However, by freeze fracture, P faces of both the axons and ensheathing cells (glia that surround the axon fascicles) contained distinctive linear arrays of particles, aligned along the small columns of extracellular space. In axons, few intramembranous particles were present outside of these arrays. Multi-helix proteins, including ion channels and connexin hemichannels, have been shown to be visible as particles by freeze fracture. This suggests that the proteins important for signal transmission are confined to the linear arrays. Such an arrangement would facilitate ephaptic transmission, calcium waves, current oscillations, and paracrine communication and may be important for olfactory neural code processing.

Keywords

freeze fracture; ultrastructure; olfactory bulb; ephaptic; connexins; hemichannels

Olfactory receptor neurons project from the olfactory epithelium to the olfactory bulb by dense bundles of thin, unmyelinated olfactory axons (Marin-Padilla and Amieva, 1989; Daston et al., 1990; Mori, 1993). The high packing density of these axons and the absence of intervening glia suggest that olfactory coding may be affected by axoaxonal interactions.

We recently demonstrated (Bokil et al., 2001) that neighboring axons are able to influence each other by ephaptic interactions—current spread through the small extracellular space. We have argued (Bokil et al., 2001) that ephaptic interactions, as well as interneuronal interactions mediated by extruded potassium ions (Bliss and Rosenberg, 1979), are important determinants

*Correspondence to: Department of Anatomy & Neurobiology, University of Maryland School of Medicine, 685 W. Baltimore Street, Baltimore, MD 21201. akeller@umaryland.edu.
Drs. Karen J. Blinder and David W. Pumplin contributed equally to this article.

of olfactory coding mechanisms. Here we test the hypothesis that gap junctions may facilitate axo-axonal communication between olfactory neurons. Two lines of evidence support this hypothesis.

First, olfactory receptors of mature mammals are constantly regenerated (Graziadei and Graziadei, 1979; Graziadei and Monti Graziadei, 1983), and developing neurons of the central nervous system are often extensively coupled by gap junctions (reviewed in Kandler and Katz, 1995; Naus and Bani-Yaghoub, 1998; Chang and Balice-Gordon, 2000). Second, olfactory receptor neurons express connexins, the proteins that form gap junctions. Olfactory receptor neurons express mRNA for connexins 43 (Zhang et al., 2000), 45 (Zhang and Restrepo, 2002), and 36 (Zhang and Restrepo, 2003). Furthermore, in immunohistochemical studies for connexin proteins, the olfactory nerve layer of the main olfactory bulb stains intensely for connexin 43 (Paternostro et al., 1995), and possibly also connexin 36 (Zhang and Restrepo, 2003; but see Belluardo et al., 2000). Although these findings suggest that connexin proteins are expressed in the olfactory nerve layer, axonal gap junctions have not been reported to occur in this layer in previous transmission electron microscopy (TEM) studies (Andres, 1969; Berger, 1969; Doucette, 1984; Marin-Padilla and Amieva, 1989; Au et al., 2002). The only gap junctions known to exist in the olfactory nerve layer are between ensheathing cells, the glia that enwrap bundles of axons (Berger, 1969; Mack and Wolburg, 1986).

The definitive method for detecting small gap junctions, freeze fracture, has not been applied to olfactory axons of the olfactory nerve layer. Freeze-fracture studies have been performed in the olfactory epithelium and a number of these studies have reported gap junctions between supporting cells, but not between olfactory sensory neurons (Kerjaschki and Horander, 1976; Usukura and Yamada, 1978; Miragall and Mendoza, 1982; Miragall et al., 1984).

The presence of connexin protein in the olfactory nerve layer and in the olfactory receptor neurons led us to hypothesize that the olfactory axons may form small gap junctions that would be visible only in freeze-fracture preparations. In the present study, we used a combined approach of freeze fracture and TEM to examine olfactory axons of olfactory nerve layer in the main olfactory bulb.

In a recent abstract (Blinder et al., 2001) we described preliminary findings suggesting that gap junctions may exist among olfactory axons, as well as between axons and their surrounding glia. In the present study, we completed extensive analyses of additional freeze fracture and TEM data and conclude that our previous conclusion was in error. We find no evidence for gap junctions involving olfactory axons, although we do confirm the presence of extensive gap junctions between ensheathing cells.

Instead, we note the presence of distinctive loose linear arrays of particles in regions where axons and glia contact the small extracellular space. We argue that these arrays, which may include ion channels and connexin hemichannels, may be involved in interneuronal communication, oscillatory activity, and volume transmission, and may be important for initial olfactory signal code processing.

MATERIALS AND METHODS

General reagents were obtained from Fisher Scientific (Fair Lawn, NJ). Aldehydes, osmium tetroxide, propylene oxide, Aclar® (Honeywell, Philadelphia, PA), and general electron microscopy and photographic supplies were obtained through Electron Microscopy Sciences (Fort Washington, PA). Lead citrate solution was from Leica Camera (Northvale, NJ). Embed812® epon resin was purchased from Ted Pella (Redding, CA). All animals except for the knockout mice and their littermates were obtained through Charles River Laboratories (Wilmington, MA). The connexin 36 knockout mice (Cx-36 KO), which express β-

galactosidase in the place of connexin 36, were from the laboratory of D.L. Paul (Deans et al., 2001). All procedures were performed under protocols approved by the University of Maryland, Baltimore Institutional Animal Care and Use Committee and according to NIH guidelines.

TEM

Seven Sprague-Dawley (SD) rats, one Wistar rat, two CD1 mice, two C57Bl6/J connexin 36 knockout mice (Cx-36 KO), and five wild-type C57Bl6/J mice (including two littermates of the knockout mice) were examined. The connexin-36 knockout mice and their littermates were adult females. All other animals were adult males. Rats weighed 200–300 g; mice were 12 weeks old.

Animals were anesthetized with 50 mg/kg sodium pentobarbital, i.p., perfused via the heart for 3 minutes with Dulbecco's phosphate-buffered saline, pH 7.2 (PBS; 20 ml/min for rats, 2 ml/min for mice), then perfused for 20 minutes with fixative. Because fixation protocols may affect the appearance of inter-axonal appositions (see below), we tested five different fixative solutions:

1. 2.0% glutaraldehyde, 0.5% paraformaldehyde, in PB, pH 7.4. This fixative was used for two SD rats, the Wistar rat, the two CD1 mice, the two Cx-36 KO mice, and four wild-type C57Bl6/J mice, including the two littermates of the knockouts.
2. 4% paraformaldehyde, 2.5% acrolein in PB (2 SD rats).
3. 200 ml of 1.25% glutaraldehyde, 1% paraformaldehyde in PB followed by 300 ml of 2.15% glutaraldehyde, 2.15% paraformaldehyde in PB (2 SD rats).
4. 2.0% glutaraldehyde in PB (2 C57Bl6/J mice).
5. 4% paraformaldehyde in PB (1 C57Bl6/J mouse).

Rats fixed using acrolein were subsequently perfused for 5 minutes with Dulbecco's PBS. Olfactory bulbs were removed, postfixed 1 hour in the same fixative (except when acrolein was used), rinsed in PBS, and 50 μm sagittal sections were cut with a Vibratome® (Technical Products Intl., St. Louis, MO). Sections were stained for 20 minutes in 0.2% osmium tetroxide and 2.3% potassium dichromate in PB; 20 minutes in 1% osmium tetroxide in PB, rinsed repeatedly in PB, and left overnight at 4°C in the final rinse. All other steps were carried out at room temperature.

The next day, sections were stained for 2 hours in the dark in 1% uranyl acetate in 70% methanol. Sections were dehydrated through a graded alcohol series followed by propylene oxide, flat embedded in epon resin, and cured overnight at 60°C under vacuum. Areas of interest were reembedded in Beem capsules. Silver-interference sections were cut with a Sorvall® 1000 ultramicrotome (Du-Pont Instruments, Wilmington, DE), collected on uncoated copper grids, and stained for 20 minutes in a stabilized solution of 2.7% lead citrate.

Sections were examined at 80 kV with a Philips 200 transmission electron microscope (FEI, Hillsboro, OR) at a magnification of 10,000–150,000×. Electron micrographs were obtained at 15,000–45,000× and printed with 2–10-fold enlargement. Selected negatives were digitally scanned at 600 dpi to 2400 dpi (depending on degree of enlargement desired) with a HP Scanjet XPA scanner (Hewlett-Packard, Palo Alto, CA) and a Power Macintosh computer. Image processing, performed with PhotoShop® (Adobe Systems, San Jose, CA), was limited to cropping and linear level adjustments.

Freeze fracture

Five additional adult male SD rats (300–500 g each) were perfused with 2.5% glutaraldehyde, 0.5% paraformaldehyde in PB for freeze-fracture studies. Perfusion protocol was as for TEM; postfixation was overnight. The next day tissue was rinsed in PB and 50-μm thick sections cut with a Vibratome. To study longitudinal axons, the most superficial portion of the lateral aspect of the main olfactory bulb was sectioned, while coronal sections of the anteriormost portion of the olfactory bulb were cut to study axons in cross section. These sections were cryoprotected in 33% glycerol, mounted between two specimen carriers (Bal-Tec, Manchester, NH), snap frozen in liquid freon-22, and fractured using a DA360 Double Replica Device (Balzers High Vacuum, Santa Ana, CA) in a modified Balzers BAF301 freeze-fracture machine. Complementary fracture faces were shadowed at a 45° angle with 1.4–1.7 nm of platinum, then reinforced with carbon. Replicas were floated onto distilled water, cleaned with commercial bleach followed by chromium sulfuric acid, rinsed, and mounted on formvar-coated slot grids for examination by TEM at 80 kV. Electron micrographs were taken in stereo with a 12° difference in angle and processed as detailed above.

RESULTS

Identification criteria

Established criteria were used to identify gap junctions in TEM electron micrographs (Brightman and Reese, 1969; Goodenough and Revel, 1970; McNutt and Weinstein, 1970) and in freeze-fracture replicas (Chalcroft and Bullivant, 1970; Larsen, 1977). In TEM, gap junctions present with two apposed bilayers separated by a 2–3 nm gap of constant width that may contain regularly spaced striations. Submembranous electron-dense material is usually present. Depending on the fixation protocol and extent of lead citrate staining, it has been reported that gap junctions may *appear* pentalaminar, with an electron-dense central gap, or septilaminar, with an electron lucent gap (Brightman and Reese, 1969; McNutt and Weinstein, 1970; Larsen, 1977).

In freeze fracture, gap junctions appear in P face as hexagonal arrays of P face intramembranous particles of uniform size, with a center-to-center spacing of ~7.5 nm (Chalcroft and Bullivant, 1970). The particles may be packed tightly, in crystalline arrays, or somewhat more loosely, with areas of crystalline hexagonal arrays (Larsen, 1977). The complementary E face contains a corresponding arrangement of pits.

Olfactory axons and processes belonging to ensheathing glia were identified in TEM micrographs according to previous descriptions (Andres, 1969; Berger, 1969; Doucette, 1984; Marin-Padilla and Amieva, 1989; Au et al., 2002) and were clearly differentiated (Fig. 1). Olfactory axons were 50–400 nm in diameter, round or oval in cross-section, with regularly spaced neurotubules. Their contours were very regular, both in cross-section and longitudinally. Their diameters remained constant longitudinally, except where they expanded to encompass a mitochondrion. The cytoplasm of ensheathing cells was less electron-dense than that of axons (Fig. 1a). The processes of ensheathing cells often had broadly undulating contours. In contrast to the axons, the visible portion of an ensheathing cell process within a field usually was of changing diameter along its length. Ensheathing cells enveloped bundles of axons, but rarely penetrated the bundles.

In freeze-fracture replicas, we identified axons and ensheathing cells by their profiles. We considered as axons processes of the appropriate size and uniform diameter traveling in bundles (Figs. 1b, 6). The regularly spaced microtubules seen in the cross-fractured cytoplasm of olfactory axons also identified these profiles as axons (Fig. 1b). We identified as components

of ensheathing cells large expanses of flat membrane (wider than the diameter of two axons; e.g., Fig. 5) and processes with changing diameter and undulating contours (Fig. 1b).

TEM of thin sections

Extensive gap junctions were present between ensheathing cells in both rats and mice in all strains examined. Such junctions were also present in the Cx-36 KO mice (data not shown). In fact, we did not observe any differences in anatomy or ultrastructure of the olfactory nerve layer between the Cx-36 KO mice and their wild-type littermates. In particular, there was no difference in the ultrastructure of cells, the spacing of axons, or the configuration of the extracellular space.

In tissue from animals perfused with fixative #1 (2.0% glutaraldehyde, 0.5% paraformaldehyde), we found numerous pentalaminar and occasional septilaminar close appositions between axons (Fig. 2a–c, 2d, respectively). Both typically had a periodic structure. In the pentalaminar junctions, the periodic structure took the form of striations extending across the entire junction, reminiscent of a railroad track (Fig. 2b,c). In other cases we noted a periodic beading of the central line (data not shown). In septilaminar junctions there was a periodic pattern within the gap (Fig. 2d). All three patterns have previously been reported in gap junctions (reviewed in Larsen, 1977). In both the pentalaminar and septilaminar junctions between axons we also frequently saw fibrillar material subjacent to the membrane (Fig. 2b–d). Such junctions were common in most of the samples we examined and were easy to mistake for gap junctions. Nonetheless, we have concluded for reasons detailed below that these are *not* gap junctions.

There are two types of intercellular junctions that may be confused with gap junctions: tight junctions and labile appositions (Brightman and Reese, 1969). The septilaminar junctions we observed were clearly not tight junctions, as these are invariably pentalaminar. Nor do the pentalaminar junctions appear to be tight junctions, as tight junctions usually do not have periodic striations or submembranous fibrillar material. Additionally, as noted below, we found no evidence for tight junctions by freeze fracture.

Labile appositions are a dehydration artifact that appear under many fixation procedures (Brightman and Reese, 1969). Like tight junctions, labile appositions lack periodic markings and submembranous electron-dense material. Additionally, labile appositions are typically accompanied by signs of tissue dehydration or fluid shifts, such as ruffled membranes and swollen mitochondria, which we did not note in our samples (Figs. 1a, 2a).

We remained concerned, however, by our failure to find by freeze fracture evidence for typical gap junctions between axons (see below). Moreover, we were concerned that most of the appositions we observed were pentalaminar in appearance (Fig. 2b,c), while most of the gap junctions we observed between ensheathing cells *in the same sections* were septilaminar (Fig. 3b). Furthermore, in the septilaminar appositions we did observe between axons (Fig. 2d), the gap was as wide as the bilayers, rather than the typical 2 nm spacing of gap junctions (e.g., Fig. 3b). None of the close appositions we observed between axons were as convincing as the extensive gap junctions we identified between ensheathing cells.

Because of these concerns, we examined by TEM a number of different specimens, ultimately examining 17 animals fixed with five different fixatives (see Materials and Methods). The atypical junctions were present in many of these specimens. However, in the SD rats fixed with the two-stage procedure (fixative #3), in which ultrastructure was particularly well preserved, close appositions involving axons were consistently absent, although gap junctions between ensheathing cells were observed (data not shown). The close appositions were also absent in the Wistar rat and in one C57Bl6/J mouse fixed with 2.0% glutaraldehyde, 0.5%

paraformaldehyde (fixative #1). We estimate that we examined ~3×10^5 μm^2 of tissue from these four animals without encountering any gap junctions involving olfactory axons.

In conclusion, images obtained from thin-sectioned material yielded no convincing evidence for gap junctions between olfactory axons or between olfactory axons and ensheathing cells.

Freeze fracture

It is widely recognized that gap junctions are most convincingly demonstrated in freeze-fracture replicas (Peters et al., 1991; Rash et al., 1998), where they appear as densely packed hexagonal arrays, as described above. We examined freeze-fracture replicas prepared from five SD rats following fixation with 2.5% glutaraldehyde, 0.5% paraformaldehyde. In total, we examined ~30 replicas representing an estimated 7.5×10^5 μm^2 of tissue.

Although we found large gap junctions between ensheathing cells (Fig. 3a), we found no hexagonal arrays indicative of gap junctions on olfactory axons or on ensheathing cells at their junctions with axons. Rather, careful study of stereomicrographs of complementary replicas led to a surprising finding: the intramembranous particles were largely *excluded* from areas of axo-axonal and axo-glial apposition (Figs. 4–7).

Instead, P faces of axons and ensheathing cells contained loosely organized linear arrays of heterogeneous intramembranous particles, typically 1 to 6 abreast. These arrays were found exclusively in regions where the axons contacted the longitudinal columns of inter-axonal extracellular space (Fig. 6; shown schematically in Fig. 7). Additional intramembranous particles were seen in the corresponding regions of the complementary E faces (Fig. 6). Particles varied in diameter from ~5–18 nm. We observed similar loose linear arrays in P and E faces of ensheathing cells where these apposed the longitudinal crevices of extracellular space at the edges of axon fascicles (Fig, 4; shown schematically in Fig. 7). In both axons and glia, the E face particles had the same distribution as the P face particles and were in register with them.

Axons had few particles outside the linear arrays. In contrast, in addition to the loose linear arrays, P faces of ensheathing cells had patches of heterogeneous intramembranous particles (Fig. 5), as well as the gap junctions already noted (Fig. 3a).

DISCUSSION

By freeze fracture and TEM, extensive gap junctions were observed between ensheathing cells of rats, confirming earlier findings (Berger, 1969; Mack and Wolburg, 1986). Similar junctions were also observed by TEM in the Cx-36 KO mice. Thus, these gap junctions must be comprised of other connexins. That is not surprising, as connexin 36 is predominantly or exclusively found in neurons (Condorelli et al., [1998], 2000; Belluardo et al., 2000; Rash et al., 2001), and connexin 43 is known to be present in the olfactory nerve layer (Paternostro et al., 1995).

In contrast to the findings with ensheathing cells, we conclude, based on TEM findings and freeze-fracture results, that gap junctions involving olfactory axons of the main olfactory bulb of rat and mouse are either nonexistent or very small and extremely rare. The close appositions we observed by TEM in some tissues, appositions that in some respects resembled gap junctions, appear to have been a fixation artifact, as they were consistently absent from the best-preserved samples. However, we remain puzzled by the periodicity frequently present in these apparent artifacts but not typically present in the artifact known as a labile apposition (Brightman and Reese, 1969). Andres (1969) also observed atypical lamellar close appositions between olfactory axons, but did not mention any periodic elements in this junction.

Freeze fracture findings confirmed that the appositions we observed are not gap junctions. Rather, intramembranous particles were conspicuously absent from areas of apposition involving axons (Figs. 6, 7). Instead, the heterogeneous axonal intramembranous particles were largely confined to distinctive loose linear arrays, found exclusively where the axons contacted the inter-axonal columns of extracellular space. Heterogeneous linear arrays of particles occurred also on ensheathing cell membranes adjacent to the extracellular spaces at the boundaries of axon fascicles (Figs. 4, 7).

We consider it unlikely that these linear arrays are an artifact of shadow angle. First, they were present in both halves of complementary replicas, although there were many more particles in P faces than in E faces, as is normal. Second, there were a few intramembranous particles present in troughs located outside of these arrays, enough to convince us that particles in the troughs were receiving shadowing.

It has been shown that large proteins appear in freeze fractures as particles having cross-sectional areas that vary linearly with the number of membrane-spanning helices, by a factor of 1.4 nm^2 per helix (Eskandari et al., 1998). In the same study, connexin hemichannels, ion channels, a water channel, and a co-transporter were all visible by freeze fracture. From the size relationship, proteins with only one or two transmembrane segments would not be visible as intramembranous particles. Large receptors are also visible as intramembranous particles (e.g., Cohen and Pumplin, 1979; Pumplin and Drachman, 1983; Kaufmann et al., 2002), as are the sodium channels of neurons and the sodium-potassium ATPase (Pumplin and Fambrough, 1983). Taken together, the results suggest: 1) that IMP in olfactory nerves may represent ion channels, ion pumps, or other large, multi-helix proteins; and 2) that IMPs are all aligned in membranes facing the small longitudinal columns of extracellular fluid that separate the axons.

The concentration of ion channels and other multi-helix membrane proteins in a relatively small space between axons could facilitate ephaptic interactions (Bokil et al., 2001), spreading calcium waves (Cinelli and Salzberg, 1992), potassium ion fluxes (Bliss and Rosenberg, 1979), current oscillations (Stopfer et al., 1997), and paracrine communication. The extracellular material we observed between axons (Fig. 1a), also observed by others (Berger, 1969), could, by its location, further restrict the effective space, partially segregating the columns of extracellular fluid from one another and restricting molecular diffusion (Boubriak et al., 2000; Nicholson et al., 2000; Tannock et al., 2002).

It is also possible that connexins, expressed by olfactory receptor neurons (Zhang et al., 2000; Zhang and Restrepo, 2002, 2003), and present in olfactory nerve layer (Paternostro et al., 1995; Zhang and Restrepo, 2003), are among the particles in these arrays. Previous TEM and freeze-fracture studies have shown definitively that the olfactory *epithelium* of mammals lacks gap junctions involving olfactory receptor neurons (Andres, 1969; Pinching and Powell, 1971a,[b]; Kerjaschki and Horander, 1976; Menco, 1980[a–d]; Miragall et al., 1994, 1996). Nor have such junctions previously been reported in axons of the *olfactory nerve layer* in TEM studies (Andres, 1969; Berger, 1969; Doucette, 1984; Au et al., 2002). The present freeze-fracture study confirms that gap junctions involving olfactory axons are not present at this level. To our knowledge, the *glomerular layer* has not been studied by freeze fracture, but in TEM studies of thin sections no gap junctions involving olfactory axons were found (Pinching and Powell, 1971a,b). It would appear, therefore, that although they express connexin proteins (see above), olfactory axons do not form gap junctions.

It is possible, however, that connexins may be present in the form of hemichannels. For example, connexin 43 is known to form functional hemichannels (Li et al., 1996). Connexin 43 hemichannels, gated by calcium (Buck, 1996; Li et al., 1996; Quist et al., 2000; Bruzzone et al., 2001), permit passage not only of ions but also of the paracrine signaling molecule NAD

+ (Bruzzone et al., 2001). The NAD+ released through the hemichannels can be converted by the ectoenzyme CD38 into the second messenger cyclic ADP-ribose, which in turn releases intracellular calcium (Bruzzone et al., 2001). Such a paracrine mechanism has been demonstrated in astrocyte-to-neuron signaling (Verderio et al., 2001). It is noteworthy that the olfactory system has the highest level in the brain of the first enzyme in the pathway for converting tryptophan to NAD+ (Foster et al., 1986), while CNS glia have been shown to contain CD38 (Pawlikowska et al., 1996).

Communication between olfactory neurons could serve different purposes at different locations within the olfactory nerve and the olfactory bulb. In the olfactory epithelium, olfactory receptor neurons with a given specificity are dispersed (Buck, 1993) within one of four expression zones (Ressler et al., 1993), so that neighboring receptors are of unrelated specificity. As they proceed toward the bulb, the axons form fascicles that repeatedly interweave and regroup (Mori, 1993). Ultimately, axons of like specificity converge on four glomeruli, one on each side of each bulb (Yoshihara and Mori, 1997). Axons with closely related specificities are targeted to glomeruli that are in close proximity to one another (Tsuboi et al., 1999). Thus, initially in its course, an olfactory axon is surrounded by axons of different specificities from its own; late in its course it is surrounded by axons of related specificities, and at the very end of its course it is surrounded by axons of identical specificity.

One can envision a hierarchical arrangement of interactions between axons in the olfactory nerve layer. Intracellular messengers would be active only in individual axons; paracrine interactions, facilitated by the distribution of the large proteins along the small extracellular spaces, would affect only axons in close proximity; ephaptic interactions (Bokil et al., 2001) would extend through-out a small fascicle; and calcium waves and current oscillations could extend throughout large areas of the nerve layer. With regard to the last, the extensive gap junctions between ensheathing cells could effectively make them a functional unit, together able to contact a large proportion of the axons and therefore able to coordinate widespread changes in neuronal excitability. Oscillatory activity, present in both olfactory epithelium and bulb, and coordinated between them (Dorries and Kauer, 2000), may be important in odor quality encoding (Stopfer et al., 1997).

The hierarchical system of axo-axonal communications proposed, combined with the sorting and re-sorting of axons along their course, would provide the flexibility needed to permit the olfactory nerve to accomplish the first stages of olfactory signal processing, including initial amplification, integration, and refinement. Further signal processing certainly occurs in the glomeruli and at the mitral cell layer (Mori and Shepherd, 1994). The relative importance of axo-axonal integration in olfactory neural code processing remains to be determined, but clearly the anatomical substrates are present to permit the axons to play an important role.

Acknowledgments

We thank Drs. Charles Greer, John Rash, Diego Restrepo, and Chunbo Zhang for helpful comments and discussion.

Grant sponsor: National Institutes of Health; Grant number: NS-31078, NS-35360 (A.K.); Grant number: GM-37751 (D.L.P.); Grant sponsor: U.S. Public Health Service; Grant number: training grant DC-00054 (K.B.).

LITERATURE CITED

Andres KH. The olfactory epithelium of the cat. Z Zellforsch Mikrosk Anat 1969;96:250–274. [PubMed: 4890668]

Au WW, Treloar HB, Greer CA. Sublaminar organization of the mouse olfactory bulb nerve layer. J Comp Neurol 2002;446:68–80. [PubMed: 11920721]

Belluardo N, Mudo G, Trovato-Salinaro A, Le Gurun S, Charollais A, Serre-Beinier V, Amato G, Haefliger JA, Meda P, Condorelli DF. Expression of connexin36 in the adult and developing rat brain. Brain Res 2000;865:121–138. [PubMed: 10814742]

Berger B. Ultrastructure of the superficial layer of the main olfactory bulp in the rabbit. Arch Anat Microsc Morphol Exp 1969;58:41–61. [PubMed: 5347112]

Blinder K, Thompson AJ, Pumplin D, Keller A. Gap junctions and their proteins in the mammalian olfactory nerve. Soc Neurosci Abstr 2001;27:1637.

Bliss TV, Rosenberg ME. Activity-dependent changes in conduction velocity in the olfactory nerve of the tortoise. Pflugers Arch 1979;381:209–216. [PubMed: 574630]

Bokil H, Laaris N, Blinder K, Ennis M, Keller A. Ephaptic interactions in the mammalian olfactory system. J Neurosci 2001;21:RC173. [PubMed: 11588203]

Boubriak OA, Urban JP, Akhtar S, Meek KM, Bron AJ. The effect of hydration and matrix composition on solute diffusion in rabbit sclera. Exp Eye Res 2000;71:503–514. [PubMed: 11040086]

Brightman MW, Reese TS. Junctions between intimately apposed cell membranes in the vertebrate brain. J Cell Biol 1969;40:648–677. [PubMed: 5765759]

Bruzzone S, Guida L, Zocchi E, Franco L, De Flora A. Connexin 43 hemi channels mediate Ca2+-regulated transmembrane NAD+ fluxes in intact cells. FASEB J 2001;15:10–12. [PubMed: 11099492]

Buck LB. Receptor diversity and spatial patterning in the mammalian olfactory system. Ciba Found Symp 1993;179:51–64. discussion 64–67, 88–96. [PubMed: 8168382]

Buck LB. Information coding in the vertebrate olfactory system. Annu Rev Neurosci 1996;19:517–544. [PubMed: 8833453]

Chalcroft JP, Bullivant S. An interpretation of liver cell membrane and junction structure based on observation of freeze-fracture replicas of both sides of the fracture. J Cell Biol 1970;47:49–60. [PubMed: 4935338]

Chang Q, Balice-Gordon RJ. Gap junctional communication among developing and injured motor neurons. Brain Res Brain Res Rev 2000;32:242–249. [PubMed: 10751674]

Cinelli AR, Salzberg BM. Dendritic origin of late events in optical recordings from salamander olfactory bulb. J Neurophysiol 1992;68:786–806. [PubMed: 1432048]

Cohen SA, Pumplin DW. Clusters of intramembrane particles associated with binding sites for alpha-bungarotoxin in cultured chick myotubes. J Cell Biol 1979;82:494–516. [PubMed: 479313]

Condorelli DF, Parenti R, Spinella F, Salinaro A Trovato, Belluardo N, Cardile V, Cicirata F. Cloning of a new gap junction gene (Cx36) highly expressed in mammalian brain neurons. Eur J Neurosci 1998;10:1202–1208. [PubMed: 9753189]

Condorelli DF, Belluardo N, Trovato-Salinaro A, Mudo G. Expression of Cx36 in mammalian neurons. Brain Res Brain Res Rev 2000;32:72–85. [PubMed: 10751658]

Daston MM, Adamek GD, Gesteland RC. Ultrastructural organization of receptor cell axons in frog olfactory nerve. Brain Res 1990;537:69–75. [PubMed: 2085790]

Deans MR, Gibson JR, Sellitto C, Connors BW, Paul DL. Synchronous activity of inhibitory networks in neocortex requires electrical synapses containing connexin36. Neuron 2001;31:477–485. [PubMed: 11516403]

Dorries KM, Kauer JS. Relationships between odor-elicited oscillations in the salamander olfactory epithelium and olfactory bulb. J Neurophysiol 2000;83:754–765. [PubMed: 10669491]

Doucette JR. The glial cells in the nerve fiber layer of the rat olfactory bulb. Anat Rec 1984;210:385–391. [PubMed: 6507903]

Eskandari S, Wright EM, Kreman M, Starace DM, Zampighi GA. Structural analysis of cloned plasma membrane proteins by freeze-fracture electron microscopy. Proc Natl Acad Sci USA 1998;95:11235–11240. [PubMed: 9736719]

Foster AC, White RJ, Schwarcz R. Synthesis of quinolinic acid by 3-hydroxyanthranilic acid oxygenase in rat brain tissue in vitro. J Neurochem 1986;47:23–30. [PubMed: 2940338]

Goodenough DA, Revel JP. A fine structural analysis of intercellular junctions in the mouse liver. J Cell Biol 1970;45:272–290. [PubMed: 4105112]

Graziadei PP, Graziadei GA. Neurogenesis and neuron regeneration in the olfactory system of mammals. I. Morphological aspects of differentiation and structural organization of the olfactory sensory neurons. J Neurocytol 1979;8:1–18. [PubMed: 438867]

Graziadei PP, Monti Graziadei AG. Regeneration in the olfactory system of vertebrates. Am J Otolaryngol 1983;4:228–233. [PubMed: 6353965]

Kandler K, Katz LC. Neuronal coupling and uncoupling in the developing nervous system. Curr Opin Neurobiol 1995;5:98–105. [PubMed: 7773012]

Kaufmann R, Junker U, Nuske K, Westermann M, Henklein P, Scheele J, Junker K. PAR-1- and PAR-3-type thrombin receptor expression in primary cultures of human renal cell carcinoma cells. Int J Oncol 2002;20:177–180. [PubMed: 11743661]

Kerjaschki D, Horander H. The development of mouse olfactory vesicles and their cell contacts: a freeze-etching study. J Ultrastruct Res 1976;54:420–444. [PubMed: 1255843]

Larsen WJ. Structural diversity of gap junctions. A review. Tissue Cell 1977;9:373–394.

Li H, Liu TF, Lazrak A, Peracchia C, Goldberg GS, Lampe PD, Johnson RG. Properties and regulation of gap junctional hemichannels in the plasma membranes of cultured cells. J Cell Biol 1996;134:1019–1030. [PubMed: 8769424]

Mack A, Wolburg H. Heterogeneity of glial membranes in the rat olfactory system as revealed by freeze-fracturing. Neurosci Lett 1986;65:17–22. [PubMed: 3703378]

Marin-Padilla M, Amieva MR. Early neurogenesis of the mouse olfactory nerve: Golgi and electron microscopic studies. J Comp Neurol 1989;288:339–352. [PubMed: 2794142]

McNutt NS, Weinstein RS. The ultrastructure of the nexus. A correlated thin-section and freeze-cleave study. J Cell Biol 1970;47:666–688. [PubMed: 5531667]

Menco BP. Qualitative and quantitative freeze-fracture studies on olfactory and nasal respiratory structures of frog, ox, rat, and dog. I. A general survey. Cell Tissue Res 1980a;207:183–209. [PubMed: 6966972]

Menco BP. Qualitative and quantitative freeze-fracture studies on olfactory and nasal respiratory epithelial surfaces of frog, ox, rat, and dog. II. Cell apices, cilia, and microvilli. Cell Tissue Res 1980b;211:5–29. [PubMed: 6967758]

Menco BP. Qualitative and quantitative freeze-fracture studies on olfactory and nasal respiratory epithelial surfaces of frog, ox, rat, and dog. III. Tight-junctions. Cell Tissue Res 1980c;211:361–373. [PubMed: 6968243]

Menco M. Qualitative and quantitative freeze-fracture studies on olfactory and respiratory epithelial surfaces of frog, ox, rat, and dog. IV. Ciliogenesis and ciliary necklaces (including high-voltage observations). Cell Tissue Res 1980d;212:1–16. [PubMed: 6969117]

Miragall F, Mendoza AS. Intercellular junctions in the rat vomeronasal neuroepithelium: a freeze-fracture study. J Submicrosc Cytol 1982;14:597–605. [PubMed: 7143514]

Miragall F, Breipohl W, Naguro T, Voss-Wermbter G. Freeze-fracture study of the plasma membranes of the septal olfactory organ of Masera. J Neurocytol 1984;13:111–125. [PubMed: 6707707]

Miragall, F.; Kremer, M.; Dermietzel, R. Intercellular communication via gap junctions in the olfactory system. In: Kurihara, K.; Suzuki, N.; Ogawa, H., editors. Olfaction and taste XI. Springer; Tokyo: 1994. p. 32-35.

Miragall, F.; Traub, O.; Dermietzel, R. Gap junction expression in the olfactory system. In: Spray, DC.; Dermietzel, R., editors. Gap junctions in the nervous system. R.G. Landes; New York: 1996. p. 243-260.

Mori K. Molecular and cellular properties of mammalian primary olfactory axons. Microsc Res Tech 1993;24:131–141. [PubMed: 8457725]

Mori K, Shepherd GM. Emerging principles of molecular signal processing by mitral/tufted cells in the olfactory bulb. Semin Cell Biol 1994;5:65–74. [PubMed: 8186397]

Naus CC, Bani-Yaghoub M. Gap junctional communication in the developing central nervous system. Cell Biol Int 1998;22:751–763. [PubMed: 10873289]

Nicholson C, Chen KC, Hrabetova S, Tao L. Diffusion of molecules in brain extracellular space: theory and experiment. Prog Brain Res 2000;125:129–154. [PubMed: 11098654]

Paternostro MA, Reyher CK, Brunjes PC. Intracellular injections of lucifer yellow into lightly fixed mitral cells reveal neuronal dyecoupling in the developing rat olfactory bulb. Brain Res Dev Brain Res 1995;84:1–10.

Pawlikowska L, Cottrell SE, Harms MB, Li Y, Rosenberg PA. Extracellular synthesis of cADP-ribose from nicotinamide-adenine dinucleotide by rat cortical astrocytes in culture. J Neurosci 1996;16:5372–5381. [PubMed: 8757250]

Peters, A.; Palay, SL.; Webster, Hd. The fine structure of the nervous system: neurons and their supporting cells. Oxford University Press; New York: 1991.

Pinching AJ, Powell TP. The neuropil of the glomeruli of the olfactory bulb. J Cell Sci 1971a;9:347–377. [PubMed: 4108057]

Pinching AJ, Powell TP. The neuropil of the periglomerular region of the olfactory bulb. J Cell Sci 1971b; 9:379–409. [PubMed: 5124504]

Pumplin DW, Drachman DB. Myasthenic patients' IgG causes redistribution of acetylcholine receptors: freeze-fracture studies. J Neurosci 1983;3:576–584. [PubMed: 6827310]

Pumplin DW, Fambrough DM. (Na++ K+)-ATPase correlated with a major group of intramembrane particles in freeze-fracture replicas of cultured chick myotubes. J Cell Biol 1983;97:1214–1225. [PubMed: 6311841]

Quist AP, Rhee SK, Lin H, Lal R. Physiological role of gap-junctional hemichannels. Extracellular calcium-dependent isosmotic volume regulation. J Cell Biol 2000;148:1063–1074. [PubMed: 10704454]

Rash JE, Yasumura T, Dudek FE. Ultrastructure, histological distribution, and freeze-fracture immunocytochemistry of gap junctions in rat brain and spinal cord. Cell Biol Int 1998;22:731–749. [PubMed: 10873288]

Rash JE, Yasumura T, Dudek FE, Nagy JI. Cell-specific expression of connexins and evidence of restricted gap junctional coupling between glial cells and between neurons. J Neurosci 2001;21:1983–2000. [PubMed: 11245683]

Ressler KJ, Sullivan SL, Buck LB. A zonal organization of odorant receptor gene expression in the olfactory epithelium. Cell 1993;73:597–609. [PubMed: 7683976]

Stopfer M, Bhagavan S, Smith BH, Laurent G. Impaired odour discrimination on desynchronization of odour-encoding neural assemblies. Nature 1997;390:70–74. [PubMed: 9363891]

Tannock IF, Lee CM, Tunggal JK, Cowan DS, Egorin MJ. Limited penetration of anticancer drugs through tumor tissue: a potential cause of resistance of solid tumors to chemotherapy. Clin Cancer Res 2002;8:878–884. [PubMed: 11895922]

Tsuboi A, Yoshihara S, Yamazaki N, Kasai H, Asai-Tsuboi H, Komatsu M, Serizawa S, Ishii T, Matsuda Y, Nagawa F, Sakano H. Olfactory neurons expressing closely linked and homologous odorant receptor genes tend to project their axons to neighboring glomeruli on the olfactory bulb. J Neurosci 1999;19:8409–8418. [PubMed: 10493742]

Usukura J, Yamada E. Observations on the cytolemma of the olfactory receptor cell in the newt. 1. Freeze replica analysis. Cell Tissue Res 1978;188:83–98. [PubMed: 639099]

Verderio C, Bruzzone S, Zocchi E, Fedele E, Schenk U, De Flora A, Matteoli M. Evidence of a role for cyclic ADP-ribose in calcium signalling and neurotransmitter release in cultured astrocytes. J Neurochem 2001;78:646–657. [PubMed: 11483668]

Yoshihara Y, Mori K. Basic principles and molecular mechanisms of olfactory axon pathfinding. Cell Tissue Res 1997;290:457–463. [PubMed: 9321710]

Zhang C, Finger TE, Restrepo D. Mature olfactory receptor neurons express connexin 43. J Comp Neurol 2000;426:1–12. [PubMed: 10980480]

Zhang C, Restrepo D. Expression of connexin 45 in the olfactory system. Brain Res 2002;929:37–47. [PubMed: 11852029]

Zhang C, Restrepo D. Heterogeneous expression of connexin 36 in the olfactory epithelium and glomerular layer of the olfactory bulb. J Comp Neurol 2003;459:426–439. [PubMed: 12687708]

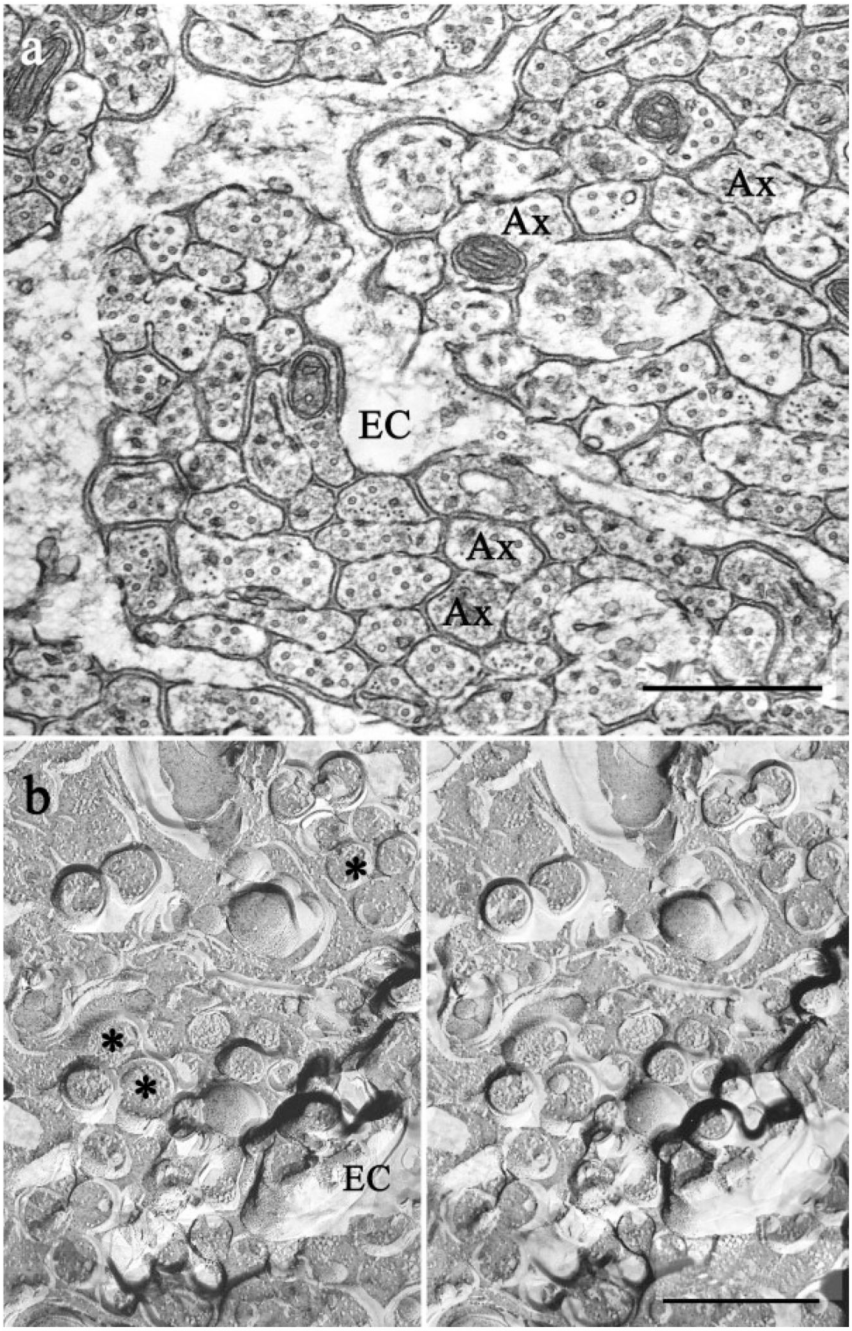

Fig. 1.

Organization of the olfactory nerve. **a:** TEM of coronal section through the olfactory nerve layer demonstrates fascicles of densely packed, small unmyelinated axons (Ax) separated by ensheathing cell glia (EC). Note the high packing density and the close appositions between the axons. **b:** Olfactory nerves visualized by freeze fracture, a technique that avoids dehydration. Stereo electron micrographs of freeze-fracture replicas confirmed that axons (asterisks) were tightly packed but without close appositions suggestive of gap junctions. Cross-fractured microtubules are prominent in axonal cytoplasm. Scale bars = 0.5 μm.

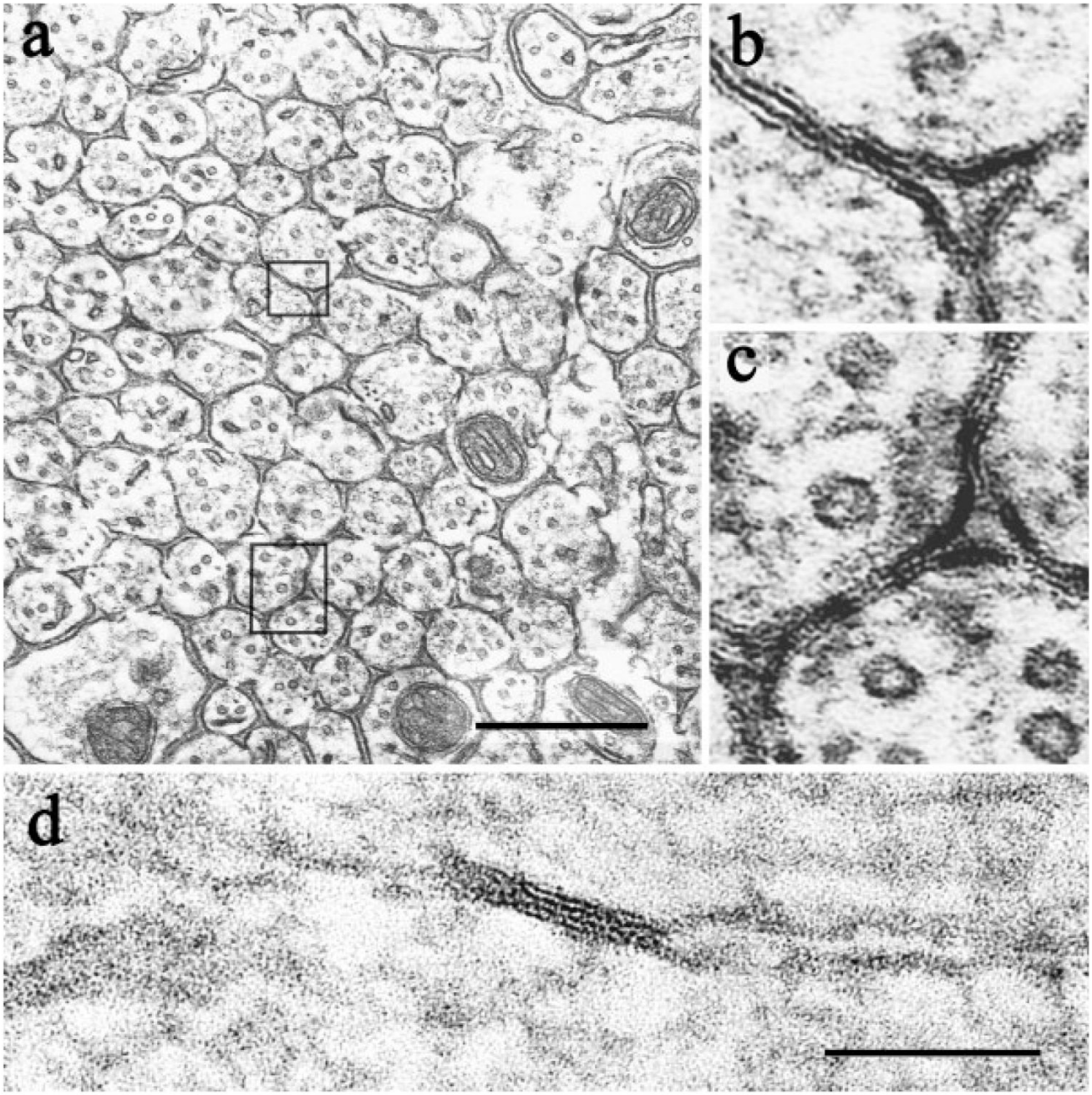

Fig. 2.

Close apposition artifacts between olfactory axons. **a–c:** Pentalaminar close appositions between axons in a coronal section through the olfactory nerve layer. Note periodic striations and submembranous fibrillar material. **d:** A septilaminar close apposition between axons in a longitudinal section. Note periodic striations across the central gap. Scale bars = 0.5 μm in a–c; 100 nm in d.

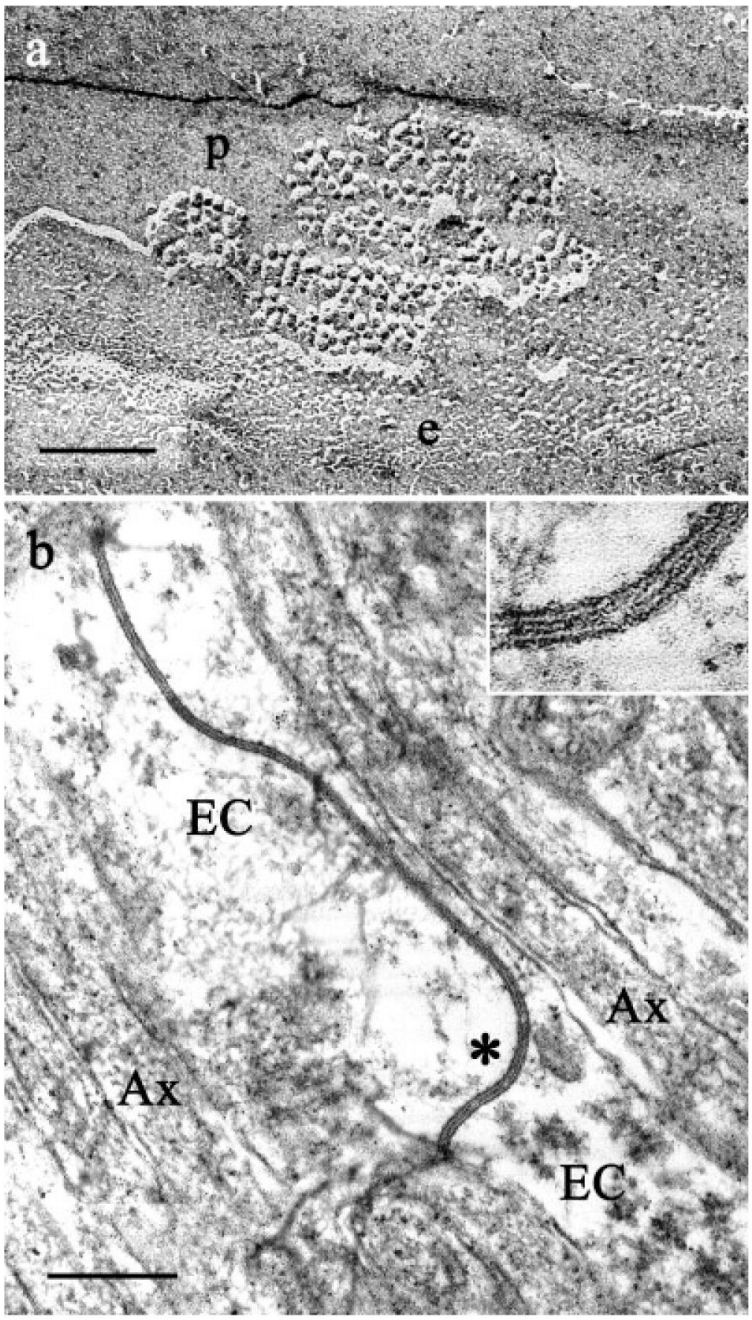

Fig. 3.

Gap junctions between ensheathing cells. **a:** Freeze-fracture replica of gap junctions between adjacent ensheathing cells. Gap junctions were identified by the typical hexagonal packing of P-face particles and E-face pits in the relatively broad, flat areas of ensheathing-cell membrane. Scale bar = 100 nm. **b:** Extensive gap junctions between ensheathing cells are apparent in ultrathin sections. Scale bar = 250 nm.

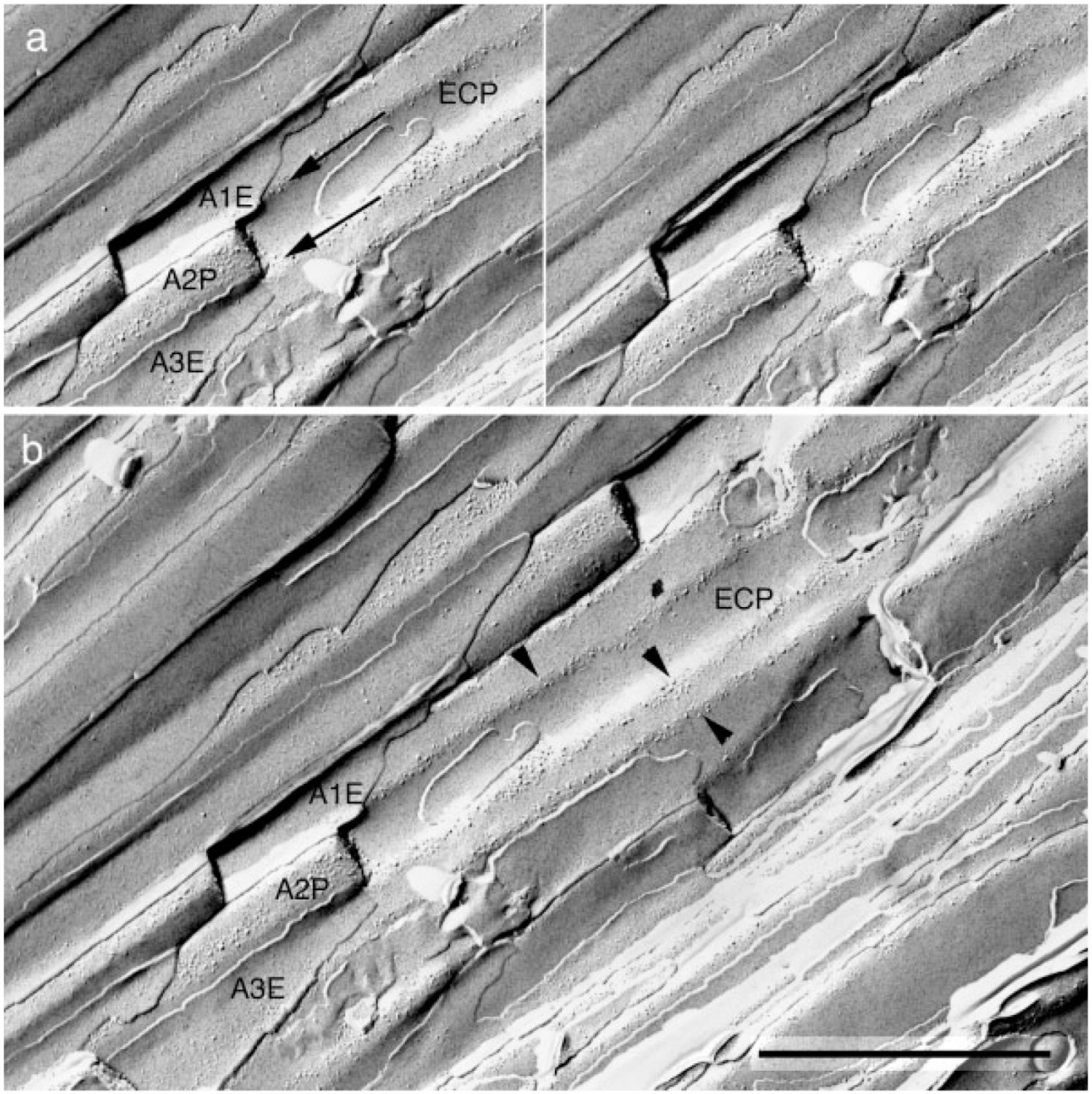

Fig. 4.

A stereomicrograph of a freeze-fracture replica from the edge of an olfactory nerve fascicle. **a:** A portion of the P face of an ensheathing cell surface (ECP) is indented by several overlying axons (A1–A3) that run parallel to each other. The fracture plane passed through the E face of axon 1 (A1E), the P face of axon 2 (A2P), and the E face of axon 3 (A3E). Ridges of the ensheathing cell (arrows) face extracellular space that lies between these adjacent axons. **b:** A more extensive view of the same field shows that intramembrane particles of the ensheathing cell are concentrated into linear arrays (arrowheads) along these ridges, while membrane area between the ridges is nearly devoid of IMP. Scale bar = 1 μm.

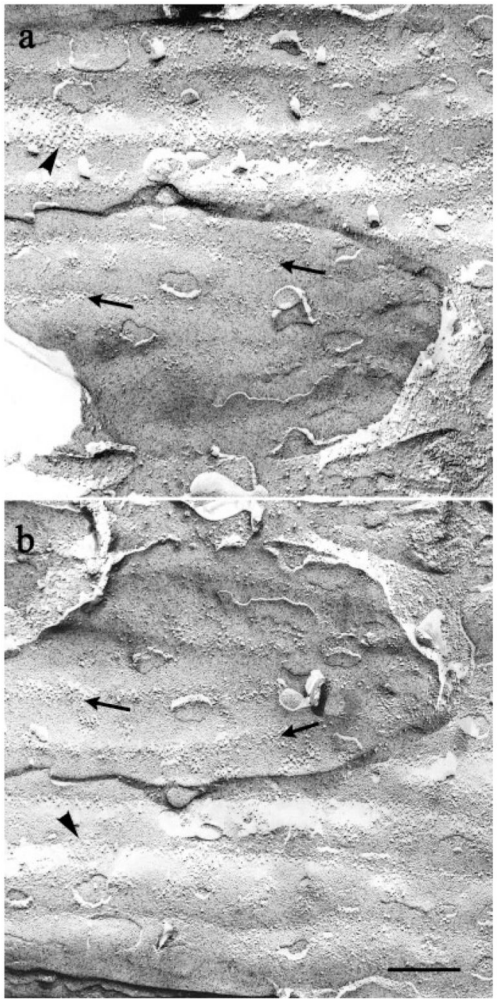

Fig. 5.

Complementary replicas of the same area of membrane of two ensheathing cells. Linear arrays of IMP lie along ridges in the P faces of both cells (thin arrow in **a**) and along the complementary indentations in the corresponding E faces (thin arrow in **b**). A few additional patches of IMP occur between the ridges in both faces (heavy arrowheads in a,b). Since the fracture plane passed through the ensheathing cell membrane, overlying axons are not seen. Scale bar = 250 nm.

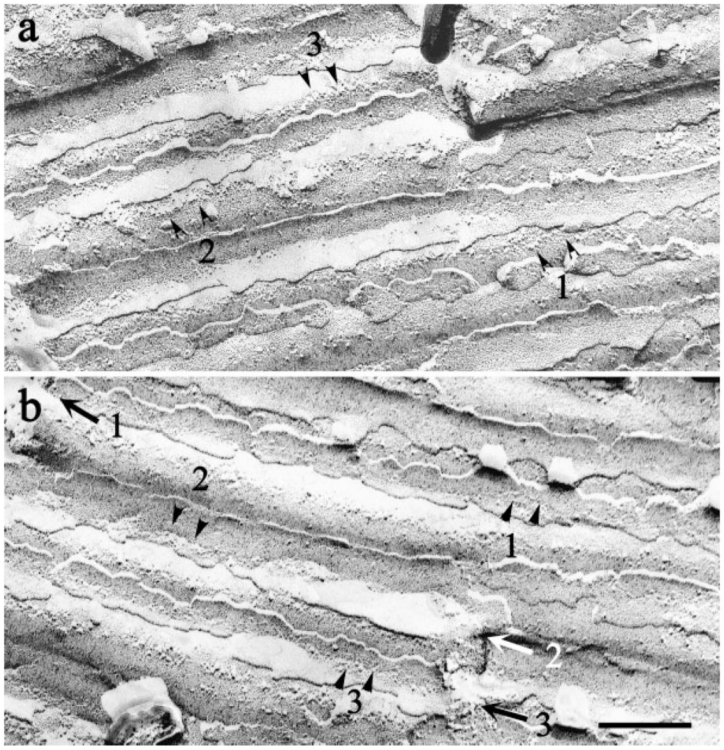

Fig. 6.

Complementary replicas of the same area of membrane of several axons. Arrowheads numbered 1–3 in b indicate boundaries between adjacent axons. Lines of IMP (numbered arrows) occur in corresponding locations of P faces (**a**) and E faces (**b**) of membrane overlying the extracellular spaces created at the boundaries between axons. Scale bar = 250 nm.

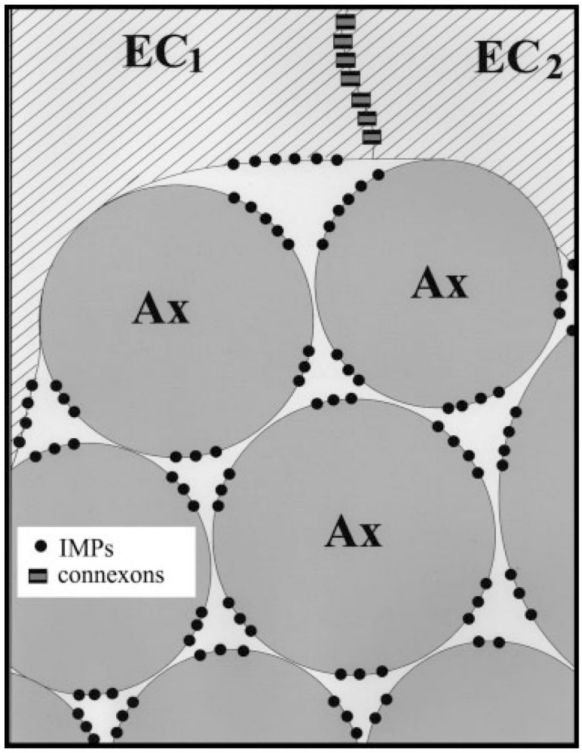

Fig. 7.

Schematic representation of the edge of an olfactory nerve fascicle. Due to cell shape and hexagonal packing, three axons (Ax) or two axons and an ensheathing cell (EC) enclose columns of extracellular space having a triangular cross-section. Intramembrane particles (black dots) are preferentially found in portions of the membrane of ensheathing cells and axons that lie adjacent to this extracellular space. Adjacent ensheathing cells are connected by gap junctions.